On the application of extended grounded slot electrodes to reduce non-circulating bearing currents

Vostrov Konstantin, Pyrhönen Juha, Niemelä Markku, Lindh Pia, Ahola Jero

DOI: 10.1109/TIE.2022.3172748

On the application of extended grounded slot electrodes to reduce non-circulating bearing currents

Konstantin Vostrov, Juha Pyrhönen, *SM, IEEE*, Markku Niemelä, Pia Lindh, *SM, IEEE*, and Jero Ahola

***Abstract*—Power-electronic-converter-induced motor bearing currents are a widespread problem in the field of electrical drives. Parasitic capacitances between the electrical machine's parts provide a path for leakage currents, which finally harm metallic ball bearings. Remembering that end-windings have a significant contribution in building up stray capacitances, a countermeasure affecting both the lamination stack and end winding areas is needed. This paper focuses on a countermeasure against the non-circulating bearing currents in the cluster of solutions at the motor side. Electrostatic shielding approach, which is a known principle to reduce capacitive couplings, is applied in electrical machines every now and then. In this work, the principle of slot-embedded grounded electrodes is extended to cover also the end-windings. Thus, the electrodes provide a better shaft-to-ground voltage mitigating effect compared to the case where electrodes are applied only in the lamination stack area. The feasibility and effectiveness of such a countermeasure are investigated. Different options in terms of scaling of both the machine size and diameter of the electrodes were analyzed and corresponding conclusions were pointed out.**

***Index Terms*— Ball bearings, electrical discharge machining bearing currents, electrical machines, finite element analysis, induction machines, variable speed drives.**

I. Introduction

IN MODERN electric drive systems, the "bearing current" phenomenon is a widespread problem causing downtimes of production. Even though the phenomenon has been known since the era of the birth of electric motors, bearing currents continue to cause inconvenience to users and compromise electric drive systems globally. The reasons for the occurrence of bearing currents can be different. In early machines, inaccurate machine geometry caused bearing currents, but after a century, the origins of the phenomenon lie in EMI and electromagnetic compatibility fields. Regardless of the origins, bearing currents degrade a machine's metallic ball bearings decreasing significantly their lifetime. Regular ball bearings are not designed for even small constant electric current passing via them and therefore the existence of parasitic currents in an electrical machine cause a bunch of problems: specific damage pattern [1] – [4], overheating, grease degradation, and loss of its chemical neutrality [2], [5], [6]; increased vibration and noise, and finally destruction of bearing balls and raceways. Even though the motor lifetime can reach 15 years or more [7] and non-stop operating intervals are declared to be as high as five years, a drive system failure because of bearing currents can occur even after one month after startup [8]. Taking into account, that in industrial operation an unplanned halt event of a single motor can cost up to 100000 USD [8] because of lost production and repair costs, the importance of the bearing current issue is hard to be overestimated.

Today, it is customary to distinguish several types of parasitic currents in electrical machines. Their classification is based on the mechanism of occurrence and the exact path of the stray current in an electrical machine. There are four types in total. All the types are described in detail both in our papers [9] – [11] and in the publications of other authors [12] – [15]. A summary table of the given types of parasitic currents is given in Table I. We see no reason to give a detailed description of these types of parasitic currents or show the current paths since an exhaustive description has been given and illustrated many times, for example, in [9], or in IEC technical specification [16]. In short, those types are the following.

Type 1: Circulating currents (also called "inductive", or "classical") arise mainly due to the asymmetry of the magnetic flux in the system. This was a frequent case in early machines. Circulating currents can also be a result of uneven distribution of the current in the stator winding, rotor eccentricity, or imprecise machine geometry [15]. Inductive bearing current forms a closed loop with a "rotor-bearing-stator-bearing-rotor" path, as shown in [10] or [11]. Modern production methods

Manuscript received November 22, 2021; revised March 12, 2022; accepted April 21, 2022. This work was supported by the Finnish Cultural Foundation's South Karelia Regional Fund under Grant 05211341.

K. Vostrov, J. Pyrhönen, M. Niemelä, P. Lindh, and J. Ahola are with LUT School of Energy Systems, LUT University, PO Box 20, 53851, Lappeenranta, Finland (e-mails: konstantin.vostrov@lut.fi, juha.pyrhonen@lut.fi, markku.niemela@lut.fi, pia.lindh@lut.fi, and jero.ahola@lut.fi).

make it possible to manufacture machine parts with sufficiently high accuracy, and thus, the given type does not currently pose the most significant danger to bearings. However, circulating currents remain a problem and still require attention in high-power AC machines [17], but this is not the subject of consideration in this article.

Type 2: Non-circulating (also "capacitive", "EDM") bearing currents are the most common type of parasitic currents in modern drive systems. This type appears in variable speed AC drive systems supplied by a frequency converter, where the output voltage is generated according to the PWM principle. The use of PWM modulation is accompanied by the common-mode voltage at the output of the converter, where the voltage waveforms consist of pulses with high du/dt values. Especially two-level converters produce high common-mode voltage output while multilevel converters have significantly reduced common-mode voltage output. However, the two-level voltage-source converter is dominating the market because of its simple and therefore economical construction.

The features mentioned above cause the appearance of the voltage between the machine rotor and stator via the machine's parasitic capacitive couplings, and finally lead to an electric current, traveling through the ball bearing. The actual bearing damage mechanism can be explained in two ways, depending on the operating mode of the machine.

At lower speed, when the lubricant film is not spread over the balls, the ball bearing shows a resistive-capacitive behavior with rapid transitions from resistive to capacitive state and back at random moments. When a galvanically conductive spot disappears due to the rotation of the balls, a micro switching arc is sparking. This arc leaves its footprint both at the raceways and the ball. Bearing material is moving, which finally results in deterioration of the affected surfaces [18] – [20].

At the rated rotational speed, when all the balls are covered with a thin oil film, the so-called Electric Discharge Machining "EDM" mechanism takes place. In this case, the bearing behaves exclusively as a capacitor, the insulation layer of which is an oil film. Together with the stator-to-rotor capacitance, which is the main energy storage for EDM, they accumulate an electric charge. As far as the oil film is thin, and dielectric properties of it are poor, the oil film breakdown occurs every moment when the voltage over the bearing reaches a threshold value (typically between 5 and 30 V, [20], [21]). At breakdown, a micro spark flashes again. The spark heats the place where it hits, melts metal, and thus surface pitting damage occurs. Keep in mind also the grease degradation caused by the flashing arc.

Due to the rapid development, high availability, and, as a consequence, extremely wide distribution of two-level-voltage-source converter-based variable speed electric drive systems, non-circulating bearing currents have become an integral part of the vast majority of new and modernized electric drive systems. Fighting against this type of parasitic current is the topic of this article.

Type 3: Stator grounding current is a leakage current through stray capacitances. It flows mainly through the "stator-to-winding" capacitance [10] and does not pose a danger to the bearings, since it does not travel through them.

Type 4: Shaft grounding current is a result of a chassis ground fault. When the stator grounding current's path is interrupted, it establishes alternative circuits to a zero potential point. In this case, a parasitic current flows from the machine case via the machine bearings to the rotor, and further via the shaft and the load's bearing, "finds" the ground through a coupled load. Moreover, if the motor ground is damaged and motor-load coupling offers a galvanic contact, the non-circulating current also acts as a shaft current, flowing through the load's bearing and damaging it.

TABLE I. DIFFERENT TYPES OF PARASITIC CURRENTS IN ELECTRICAL DRIVES OVERVIEW

Type	Origins	Stray current path
Circulating bearing currents	1) Magnetic circuit and geometry inaccuracy; 2) Uneven distribution of the current along the length of the winding as a result of capacitive leakage currents	Closed loops along the path "rotor – bearing – stator – bearing – rotor"
Non-circulating bearing currents	Common-mode voltage and high du/dt values, caused by frequency converters	Winding – rotor – bearing – stator – grounding terminal
Stator grounding current	Current leakage from the live winding via the parasitic capacitances	Winding – stator – grounding terminal
Shaft grounding current	Current leakage via the parasitic capacitances and violation of electric motor grounding with the presence of grounding of the driven load	Winding – stator – bearing – shaft – load bearing – load's grounding terminal; Winding – rotor – shaft – load bearing – load's ground;

Since this work is focused on suppressing non-circulating bearing currents, only this type will be considered further. In order to suppress the phenomenon, there are different strategies available. It is possible to reduce the common-mode voltage on the side of the frequency converter, use filters, or break the parasitic capacitive couplings on the side of the electric motor. The method described in this article belongs to the latter option - to fight with bearing currents at the side of an electric motor. In addition, it is possible to provide parasitic currents with an alternative flow path in order to exclude the bearings from the circuit or use special bearings designed to apply current through them. A detailed review of existing techniques for suppressing bearing currents was recently made in [11].

It has been theoretically and experimentally shown that breaking of stray capacitance between electrical machine parts is an effective way to fight against non-circulating bearing currents. This method has great potential for further development and represents a field for extra studies.

This paper is an evolutionary continuation of works [22] and [10], where the design and principle of using slot-opening electrodes to reduce bearing currents were described. It is an extended version of the conference paper [23], in which it was proposed to use slot-opening electrodes to reduce parasitic capacitances both in the lamination zone and in the area of the end-windings.

In the present work, the effectiveness of slot-opening electrodes is experimentally confirmed when they are extended to cover the winding overhang parts. The exact contribution of the end-windings coverage in the reduction of shaft voltage is estimated. The work also addresses the scaling questions – both of machine size and the slot-opening electrode's thickness. Finally, some specific features of the topic are highlighted.

In the current paper, the term "shaft voltage" means the voltage between the machine's shaft and the system ground.

II. THEORY BEHIND

A. Parasitic Capacitances

Looking at the structure of a regular AC motor, a set of parasitic capacitances can be observed, as shown in Fig. 1. When the motor is supplied with a balanced three-phase sine voltage, e.g., in a direct online operation, the common-mode voltage and high-frequency harmonics are absent. Under such ideal circumstances, these small capacitances cannot give any negative effect. But, when a non-sine waveform (for example, high-carrier-frequency PWM voltage waveform) meets an electric motor, a considerable part of the current starts leaking from the stator windings via these parasitic capacitances. In the context of the danger to the bearings, the most undesired case is when the parasitic current starts leaking via the winding-to-rotor capacitance C_{wr} and further passes the ball bearings (activating an EDM mechanism) on its way to the ground.

When dealing with an electrical machine's geometry, one should remember that despite the core, or lamination stack, area of an electrical machine, the end-winding area also has a considerable contribution in different effects. Considering the parasitic capacitances, it was established [24], that the winding overhang region may contribute from 35% to 40% of the total winding-to-rotor capacitance in AC machines of 500 to 0.15 kW respectively. A schematic division of the machine regions and the corresponding capacitive couplings are illustrated in Fig. 1. According to the above mentioned, it is not enough to apply electrostatic shields in the core-area only, as it was done in, i.e., [15] and [19]. In that case, the parasitic current is still able to reach the rotor and harm the bearing, albeit with a smaller amplitude. To achieve maximum non-circulating bearing current suppression effect, the capacitive coupling between the rotor and winding should be blocked completely, i.e., both in the core area and the end-winding area capacitance effect should be mitigated.

B. About Bearing Voltage Ratio

The commonly accepted indicator to measure the non-circulating bearing currents' potential impact is the Bearing Voltage Ratio, *BVR*.

The *BVR* shows the fraction of the common-mode voltage which is mirrored across the bearings' raceways. By the definition, *BVR* can be found as:

$$BVR = \frac{U_b}{U_{com}}, \tag{1}$$

where U_b is the voltage across the bearing, i.e., the voltage between the shaft and the grounding (further named also as "shaft voltage"), U_{cm} is the common-mode voltage supplied to the motor by a frequency converter. Equation (1) is valid for all cases either at theoretical or experimental stages.

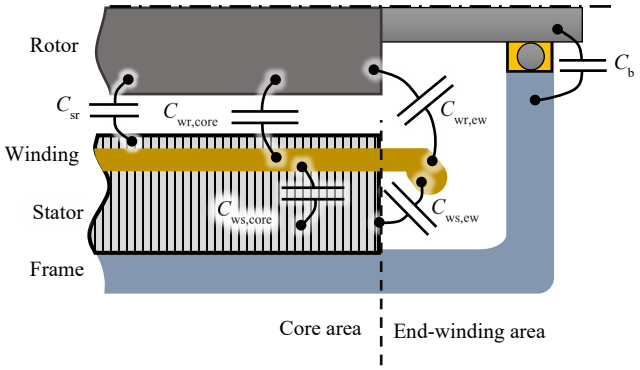

Fig. 1. Electrical machine's structure and main parasitic capacitances. The figure shows the division of an electrical machine into a "core-area" and "end-winding area". $C_{wr} = C_{wr,core} + C_{wr,ew}$ – total winding-to-rotor capacitance, $C_{ws} = C_{ws,core} + C_{ws,ew}$ – total winding-to-stator capacitance, C_{sr} – stator-to-rotor capacitance, C_b – bearing capacitance. $C_{wr,core}$ and $C_{ws,core}$ are the parts of the winding-to-rotor and winding-to-stator capacitances, formed by the core area; $C_{wr,ew,}$ and $C_{ws,ew}$ are the parts of the winding-to-rotor and winding-to-stator capacitances, formed by the end-winding area.

When an electrical machine with its parasitic capacitances is considered as a capacitive voltage divider [18], *BVR* can be found using the values of its constituent capacitances, according to the following equations. For a general case

$$BVR = \frac{C_{wr}}{C_{wr} + C_{sr} + 2C_b}, \tag{2}$$

where C_{wr} is the total winding-to-rotor capacitance, C_{sr} is the stator-to-rotor capacitance, C_{ws} is the total winding-to stator capacitance, and C_b is the bearing capacitance.

When the *BVR* is calculated for the machine equipped with slot-opening-embedded electrostatic shields (either short or extended), the following augmented equation should be used [11]:

$$BVR = \frac{C_{wr}'}{C_{wr}' + C_{sr} + 2C_b + C_{er}}, \tag{3}$$

where C_{er} is the capacitance between the slot-opening-embedded electrode and the rotor, C_{wr}', is a residue winding-to-rotor capacitance left after the slot-opening electrode is placed.

C. Safe levels of BVR

Normally, in AC machines the *BVR* is at the level of 3…10% [18], [25], and the lower the value the better.

As described below, the maximum acceptable safe level of *BVR* is averaging between 2-6% and is determined as a fraction of the voltage supplied to the electric machine. From the point of view of bearings, the voltage level between the raceways of the order of 10 volts peak and lower is considered safe. In small machines (1.5 kW or less) the maximum allowed voltage is even smaller – about 5 V peak [26]. At such a low voltage, the dielectric strength of the oil film is strong enough to prevent insulation breakdown and initiation of EDM damage. When the shaft voltage exceeds the threshold value, bearing damage occurs.

Given that the *BVR* shows the bearing voltage as a percentage of the applied voltage, the safe level of the *BVR* will naturally decrease with increasing supply voltage. For example (assuming the threshold voltage across the bearing as 10 V), for 230 V (phase to phase rated voltage) machines, the safe *BVR* will be 6.1%, for 400 V machines - 3.5%, and for 690 V - 2%. The maximum safe levels of *BVR* for the wide range of supply voltages are shown in Fig. 2.

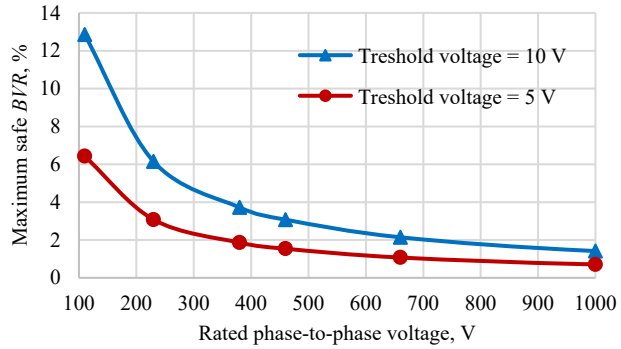

Fig. 2. Maximum safe values of *BVR* as a function of the voltage applied to the phase winding of an electrical machine.

D. The objective of the current work

The object of this study is a slot electrode system designed to reduce *BVR*. Despite the fact that the use of slot electrodes in the core area of the machine results in a significant decrease in *BVR*, in order to reliably suppress the phenomenon of bearing currents, additional measures aimed at the area of the end-windings are required.

If the shielding principle or any other countermeasure is applied exclusively to the core area, the *BVR* reduction effect may not be sufficient to achieve the aforementioned safe values. As suggested in [23], the use of such an end-winding shielding system presents a structurally simple and effective system for reducing the *BVR*. The extended slot electric system is shown in Fig. 3.

Thus, the aim of this work is to study the effect of extended grounded electrodes, their influence on the *BVR*, as well as to clarify the scaling opportunities.

III. Simulation-based study

To find parasitic capacitances, calculate *BVR*, and assess the risk of bearing damage in various machines using standard and elongated slot electrodes of various diameters, corresponding 3D models of electric machines of various capacities were analyzed.

This work covers four-pole machines with a rated power capacity of 3, 15, 30, and 110 kW. These machines were built in 3D in SolidWorks and then modeled in COMSOL environment using its Electrostatics module. The parasitic capacitances C_{wr}, C_{sr}, C_{ws}, and C_{er} were found, and the *BVR* was calculated for the original machines, and for motors with various modifications. The geometry and exact dimensions of the studied machines being modeled are schematically shown in Fig. 4 and listed in Table II.

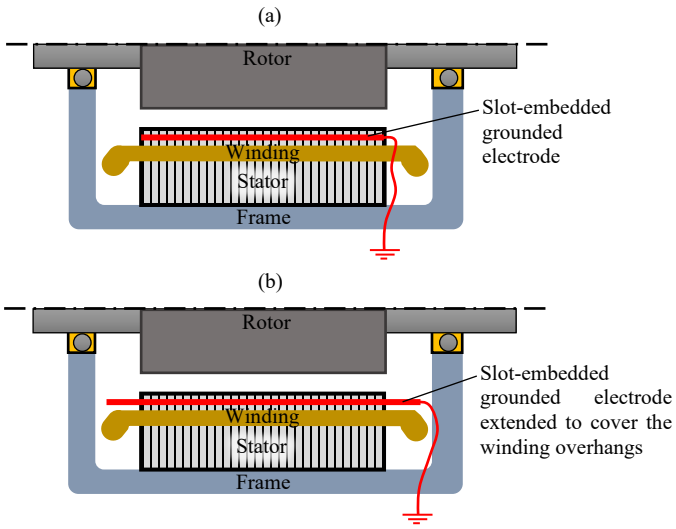

Fig. 3. The slot-embedded electrostatic sheld in a form of a single wire: a) – the electrode is placed to cover the core area only; b) – the electrode is extended to cover both core and end-winding areas.

The test motors were equipped with short and elongated slot electrodes. Each slot opening was equipped with a single electrode, the diameter of which, *d*, was also a variable parameter in the study.

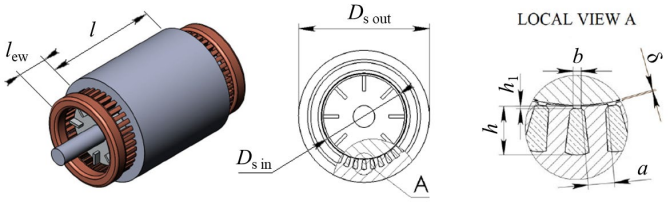

Fig. 4. The 3D model of an electrical machine being utilized in the modeling process. The model is parametrically adjustable to represent different size motors. The parameters used to model different machines are listed in Table II.

TABLE II. Main Dimensions of the Machines In the Study

Parameter, in mm	Machine rated power, kW			
	3	15	30	110
Air gap δ	0.3	0.5	0.6	0.9
Tooth width a	6.1	11	14	21.9
Slot opening width b	2.65	3.5	3.6	4.5
Shaft diameter D_{shaft}	28	42	55	80
Stator inner diameter $D_{s\,in}$	100	165.8	201.8	302.6
Stator outer diameter $D_{s\,out}$	153.9	255.4	310.5	465.5
Total height of the slot h	15.2	20	29.9	44.3
The slot height remaining above the winding h_1	0.6	1	1.1	1.7
Lamination stack length l	100	272	305	406
Winding overhang's length l_{ew}	41.5	70	81.8	112

Results of FEM-based calculation of capacitances and *BVR*s for different cases together with the list of all considered cases are shown in Table III.

This article has been accepted for publication in a future issue of this journal, but has not been fully edited. Content may change prior to final publication. Citation information: DOI 10.1109/TIE.2022.3172748, IEEE Transactions on Industrial Electronics

TABLE III. PARASITIC CAPACITANCES COMPUTED AND *BVR*S FOUND

Design	Power, kW	*d*, mm	C_{wr}, pF	C_{sr}, nF	C_{er}, nF	*BVR*	Ratio *d*/*b* [%]	Losses, mW
Original	3	-	94.7	0.72	-	11.1	-	-
	15	-	181.9	2.08	-	7.87	-	-
	30	-	182.9	2.47	-	6.74	-	-
	110	-	202.6	3.41	-	5.53	-	-
Slot-opening elect-rodes	3	0.1	74.9	0.71	0.05	8.46	3.8	0.004
		0.3	66.3	0.71	0.08	7.34	11.3	0.33
		0.5	59.0	0.71	0.11	6.32	18.9	2.31
		0.75	50.2	0.71	0.24	4.79	28.3	10.87
	15	0.1	128.8	2.07	0.11	5.45	2.9	0.01
		0.3	116.3	2.07	0.15	4.87	8.6	0.94
		0.5	105.6	2.07	0.20	4.36	14.3	6.60
		0.75	94.4	2.06	0.26	3.81	21.4	29.97
		1	86.8	2.06	0.35	3.41	28.6	81.45
	30	0.1	144.3	2.44	0.07	5.33	2.8	0.01
		0.3	118.6	2.47	0.11	4.32	8.3	0.99
		0.5	110.3	2.46	0.13	4.00	13.9	7.19
		0.75	101.5	2.46	0.17	3.65	20.8	33.77
		1	94.3	2.45	0.2	3.36	27.8	98.98
	110	0.1	151.3	3.38	0.15	4.06	2.2	0.03
		0.3	140.7	3.37	0.18	3.75	6.7	2.45
		0.5	131.4	3.37	0.22	3.48	11.1	18.01
		0.75	121.9	3.36	0.27	3.20	16.7	85.52
		1	113.9	3.35	0.33	2.95	22.2	252.73
		1.3	102.5	3.36	0.42	2.60	28.9	664.40
Extended slot-opening elect-rodes	3	0.1	71.2	0.71	0.04	8.19	3.8	0.004
		0.3	63.1	0.71	0.08	7.01	11.3	0.33
		0.5	54.8	0.71	0.12	5.88	18.9	2.32
		0.75	44.0	0.70	0.26	4.15	28.3	11.08
	15	0.1	125.9	2.06	0.11	5.35	2.9	0.01
		0.3	111.8	2.06	0.15	4.70	8.6	0.94
		0.5	98.7	2.05	0.20	4.11	14.3	6.66
		0.75	84.3	2.05	0.27	3.43	21.4	30.16
		1	72.1	2.05	0.37	2.84	28.6	81.72
	30	0.1	123.6	2.47	0.09	4.52	2.8	0.02
		0.3	111.5	2.47	0.12	4.06	8.3	1.3
		0.5	101.4	2.46	0.14	3.67	13.9	9.25
		0.75	89.6	2.46	0.18	3.22	20.8	42.26
		1	76.7	2.45	0.26	2.70	27.8	119.98
	110	0.1	152.0	3.37	0.13	4.10	2.2	0.05
		0.3	133.0	3.36	0.18	3.56	6.7	3.77
		0.5	119.5	3.36	0.23	3.18	11.1	27.56
		0.75	107.1	3.35	0.29	2.82	16.7	129.94
		1	94.3	3.34	0.35	2.45	22.2	381.28
		1.3	85.4	3.36	0.45	2.17	28.9	992.31

There are several important things to be born in mind.

Firstly, there is a physical limit of placing a certain diameter electrode into the slot opening. When placing a round slot electrode, its diameter must be less than the sum of the air gap (δ in Fig. 4) and the remaining slot opening depth (h_1 in Fig. 4). Otherwise, the slot electrode will touch the moving rotor. For the machines presented in the given paper, such limits are 0.9, 1.5, 1.8, and 2.5 mm for 3-, 15-, 30-, and 110-kW motors respectively. In reality, these numbers should be kept lower to ensure an adequate air gap between the electrode and the rotor. In the best case, to avoid any possible issues related to the reduction of the original airgap and extra windage losses, the grounded electrodes being introduced in the slot openings have to be placed below the inner surface of the stator, i.e., the diameter of the wire has to be equal or less than h_1. If the slot has a slot key, the most reliable method is to embed the electrode in the slot key.

Secondly, we have to remember, that with growing machine size its slot opening width *b* also grows. Because of that, it is not relevant to compare the effect of the same slot electrode applied in the different machines, because in a small machine a larger portion of the total slot opening area will be covered. The penultimate column in Table III is just showing that by giving us a slot opening overlapping ratio *d*/*b*. The range of electrode diameters was selected in such a way as to get an overlapping ratio *d*/*b* up to 30% for each motor under study.

Finally, for practical use, the question of possible extra losses is of interest. For the machines and cases considered in the present work, actual eddy current losses caused by slot-opening electrodes were found using 2D FEM-analysis conducted in Altair FLUX (steady-state AC magnetic application). The results are shown in the rightmost column of Table III. More considerations related to extra losses and possible other negative effects are listed in the Discussion section.

IV. LABORATORY EXPERIMENT

At the experimental stage of the work, the proposed machine modernization and effect of electrodes was tested with a four-pole 15-kW machine available in the laboratory. As the basis for the test setup, the bench described in [11] was used. The regular ball bearings were replaced with hybrid ("ceramic") ball bearings to make it possible to measure the shaft voltage.

Despite the fact that the experiment partially overlaps with the research done in [11], the main purpose and novelty of the present work lie in the study of the effects of extended slot electrodes intended to shield also the end winding. In addition, electrodes of different diameters were tested in this work – the test machine was equipped with electrode wires of the diameter of 0.3 and 0.75 mm.

Figure 5 shows the 15-kW machine in which the extended electrode concept is applied. Extended grounded electrodes create an effect of a shielding structure for the end-winding parts, similar to that proposed in [9]. At the same time, they are not a separately mounted structure and represent a single whole with the core-mounted shielding system. This simplifies the installation of such a system, improves system integrity and robustness, and reduces costs.

The schematic diagram of the experimental setup with a description of all the elements is shown in Fig. 6.

Fig. 5. The extended slot electrodes with a diameter of 0.3 mm (left) and 0.75 mm (right) are installed in a regular 15-kW induction machine.

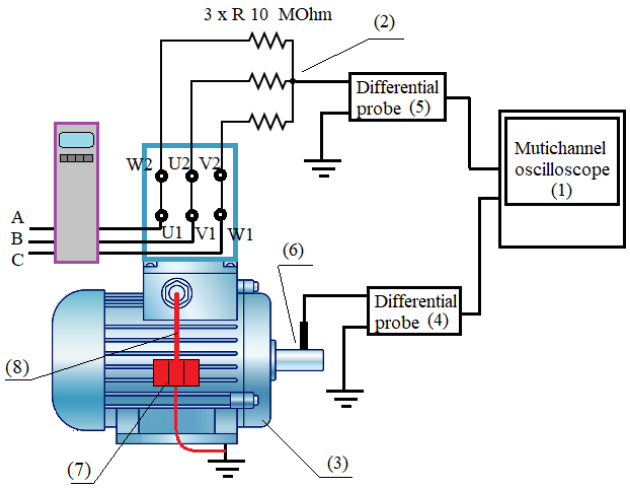

Fig. 6. Laboratory setup; 1: Yokogawa DL850 oscilloscope, 2: artificial neutral point connection, 3: 15 kW ABB industrial motor, 4: differential probe for measuring U_b, 5: differential probe for measuring U_{cm}, 6: brush connection, 7: electrodes' terminal box connected to the machine grounding, 8: a sheaf of slot electrodes, collected and taken out from the machine. The parts indicated by red show the elements added in the modified motor.

During the experiment, common-mode voltages and shaft voltages were measured to enable the finding of the *BVR* in different cases.

The common-mode voltage U_{com} is the feature of the supplying frequency converter and is not supposed to be changed case by case unless the converter type is totally changed e.g. from a two-level converter to a three-level one. The common-voltage waveform of the ABB ACS400 converter has been reported in [11]. The switching frequency of the converter used in the present study is 4 kHz.

The voltage across the bearing U_b is subject to be changed depending on the machine geometry and exact countermeasures applied to the machine. In this study, several tests representing different cases are conducted. They are all described further and listed in Table IV together with the measurement results.

TABLE IV. MEASURED VOLTAGES AND CORRESPONDING BEARING VOLTAGE RATIOS IN DIFFERENT CASES

Test #		1	2	3	4	5	6	7	8
Grounded wire placed over:	Core-area	-	+	+	-	-	-	+	+
	DE EW	-	-	+	+	+	-	+	-
	NDE EW	-	-	+	+	-	+	-	+
BVR [%]									
BVR of the original (un-modified) motor; measurement was done previously in [11]		7.12	-	-	-	-	-	-	-
Electrode diameter 0.3 mm	BVR_{RMS}	6.46	3.48	3.09	5.97	6.13	6.37	3.22	3.31
	BVR_{FFT}	6.42	3.46	3.04	5.94	6.11	6.21	3.19	3.28
	$BVR_{direct\ RMS}$	8.12	4.37	3.88	7.51	7.71	8.01	4.05	4.15
	$BVR_{direct\ FFT}$	7.94	4.27	3.75	7.34	7.56	7.67	3.94	4.05
	Average	7.23	3.89	3.44	6.69	6.88	7.06	3.60	3.70
Electrode diameter 0.75 mm	BVR_{RMS}	8.12	3.06	3.11	8.26	9.16	8.06	2.9	3.32
	BVR_{FFT}	7.9	2.14	2.08	7.48	7.49	7.61	2.13	2.32
	$BVR_{direct\ RMS}$	8.41	3.17	3.22	8.56	9.49	8.36	3.01	3.44
	$BVR_{direct\ FFT}$	8.05	2.18	2.12	7.63	7.63	7.76	2.18	2.37
	Average	8.12	2.64	2.63	7.98	8.44	7.95	2.56	2.86

The machine was prepared for an experimental study by gluing a system of extended slot electrodes. During the tests 1…8, all electrodes physically stayed in the machine. To study different cases, some parts of the system were just cut off, but not actually removed from their place. The effect of the slot electrodes being disconnected, but not extracted, was mentioned in [11], and this discussion will be continued in the current paper.

First of all, the *BVR*s of the original, i.e., unmodified motor with ceramic bearings (Test #1 in Table IV) is taken as a reference. *BVR* of out-of-shelf 15 kW motor was found previously in [11]. Test#1 was also conducted for cases with 0.3- and 0.75-mm wires. Those tests mean that *BVR*s were measured in the machines being equipped with corresponding slot electrodes, but they are disconnected from the grounding terminal.

Further, a series of tests of the motor equipped with core-area-placed slot electrodes of different diameters (Test #2 in Table IV) is conducted. The electrodes were placed as it shown in Fig. 3a, and connected and grounded according to Fig. 7h.

Then, as Test #3, the machine with extended slot electrodes is tested. In this case, long uninterrupted electrodes are placed to cover the slot openings and end windings at both ends, as shown in Fig. 3b. This case is intended to be utilized as a basic mode to provide the desired bearing currents eliminating effect. The connection of the electrodes is implemented as shown in Fig. 7h.

Finally, to understand the effect of shielding of different parts of the machine independently, several additional tests were done.

The coverage of the end windings with leaving the core-mounted part of the electrode ungrounded is tested under Test #4. The positioning of the electrodes is schematically shown in Fig. 7a, and Fig. 7b clarifies the system connection and grounding.

Covering of only drive-end winding overhang and non-drive end winding overhang are done as Test #5 (Fig. 7c) and Test #6 (Fig. 7d) respectively. The electrodes are connected and grounded using a structure shown in Fig. 7e.

Test #7 and Test#8 are conducted, when one of the drive-end and non- drive-end windings was covered together with the core-area applied electrodes. For those cases, the position of electrodes is shown in Fig. 7f and Fig. 7g. Electrodes are connected and grounded according to Fig. 7h.

As shown in Table IV, the Bearing Voltage Ratios in every test case were measured in several ways, and the average value for each row was found. All tests were conducted at the supply frequency of 20 Hz. The *BVR* was calculated in four ways (see Table IV):

$$BVR_{RMS} = U_{shaft\ RMS} / U_{cm\ RMS}$$
$$BVR_{FFT} = U_{shaft} / U_{cm}$$
$$BVR_{direct\ RMS} = U_{shaft\ RMS} / U_{cm\ direct\ RMS}$$
$$BVR_{direct\ FFT} = U_{shaft} / U_{cm\ direct},$$

where U_{shaft} and $U_{shaft\ RMS}$ are the fundamental harmonic and the RMS ("Root Mean Square") value of the shaft voltage waveform observed from the oscilloscope; U_{cm} and $U_{cm\ RMS}$ are the fundamental harmonic and the RMS value of the common-

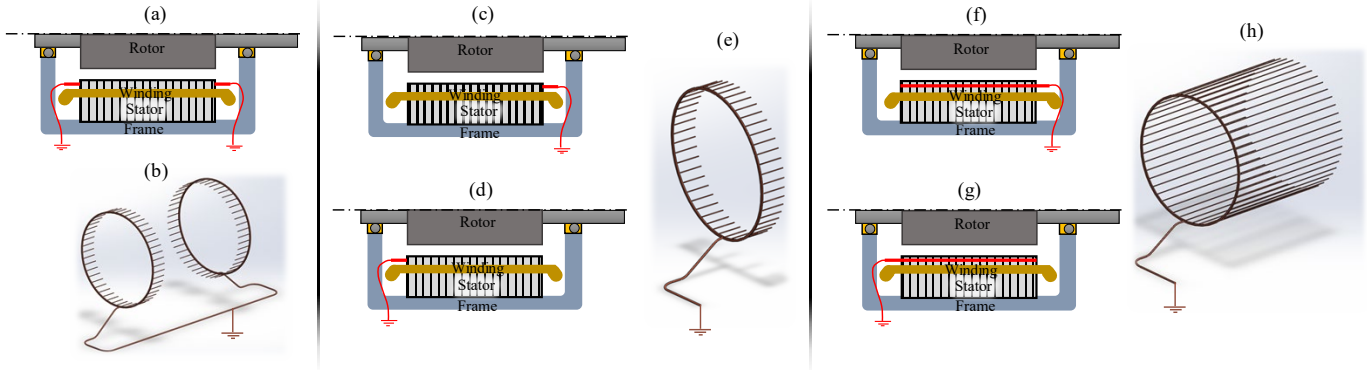

Fig. 7. The positioning of the wires and a electrodes' system sketches used in different tests: a) – a scheme of a setup to conduct Test #4; b) – 3D vizualization of the electrode systems integrated in the test motor in Test #4. The short wires are supposed to cover only the end-windings at both ends of the machine; c) and d) – position of electrodes in Test #5 and Test #6 respectively; e) – the grounded electrodes' assembly being mounted to conduct tests #5 and #6. The shown structure can be mounted either at the drive-end (to conduct Test #5) or at the non-drive-end (to conduct Test #6); f) and g) – position of slot electrodes to conduct Test #7 and Test #8 respectively; h) – the electrode assembly used in tests #7 and #8. The electrodes in Test #2 and Test #3 are connected and grounded in the same manner.

mode voltage being found via the supply voltages waveforms as $(U_U + U_V + U_W)/3$; $U_{cm\ direct}$ and $U_{cm\ direct\ RMS}$ are the fundamental harmonic and RMS value of the common-mode voltage being measured directly between the artificial neutral point (2) of Fig. 6 and the ground.

V. Discussion

The results of the FEM-based modeling are visualized and presented in Fig. 8, where we can notice that utilization of the grounded electrodes – either core-mounted or extended – has the most significant effect on the small-scale machines. Smaller machines have originally higher *BVR* and are thus more endangered with bearing currents. Since low-power electric drives often operate in the 0.4 kV class, a safe *BVR* level for them is 3-4%. Such values are barely achievable with the electrostatic shielding principle, and it is obligatory that end-windings are protected. For example, in the 3-kW machine modeled, application of the thinnest 0.1 mm wire to the core-area only gives already 23.8% reduction of *BVR* (from 11.1% to 8.46%), and a 26.3% reduction (from 11.1% to 8.18%), when extended to cover also the end-windings. Such *BVR* drop is quite significant and for sure would increase the bearing lifetime but will not eliminate the bearing currents totally. When the electrode diameter is increased to 0.75 mm, the *BVR* drops down to the values of 4.79% and 4.15%, when the electrodes are placed over the core area only and extended to the windings overhang region respectively.

On a scale of 15-30 kW, the *BVR* values of original machines are smaller – about 7-8%. But, as far as the supply voltage is higher in these machines, the target safe level of *BVR* is lower as well – around 2-3%. Here again, values below 3.4% are not available, if the end-windings are not protected. When the grounded electrodes are extended, it becomes possible to reduce *BVR* down to 2.7%, which can be considered a safe value.

In a 110-kW machine, similarly to 15-30 kW ones, the extended electrodes provide an option to reach the most effective *BVR* reduction taking the original percent value down by an extra 0.3…0.5 points.

Also, if the acceptable *BVR* value is set at a higher level, the extended electrodes help to reach the same effect with thinner wire diameter. For example, for a 110-kW machine, the *BVR* equaling 3% is reachable with 1 mm wire placed over the core-area only. But, if extended electrodes are used, a 0.6 mm wire would provide the same effect.

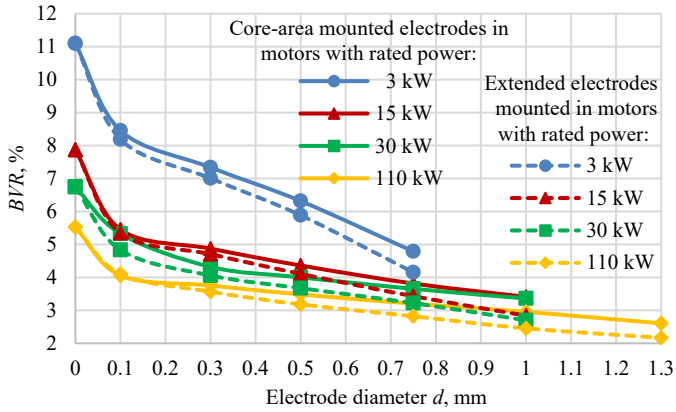

Fig. 8. Influence of the grounded slot electrodes of different diameters utilized in different size motors. Zero electrode diameter means an original unmodified machine.

Further, at the stage of an experimental study of 15-kW, the effects of the applying of different combinations of grounded electrodes were observed. The *BVR*s being measured in different cases as described in Table IV, are represented in Fig. 9.

The *BVR* values of the original 15-kW machine, and modified machines with both short and long slot electrodes are of particular interest as reference points for proofing the correctness of the FEM-computed data. The computed values are plotted in Fig. 9 over the real data. The comparison of FEM-computed *BVR* values with experimentally received ones gives us a ground to declare, that analytically found *BVR*s are overestimated in all cases. The maximum deviation of 25% for machine equipped with 0.3-mm electrodes was observed with Test #3. The machine with 0.75-mm electrodes gave maximum disaccord of 30% in Test #2.

This article has been accepted for publication in a future issue of this journal, but has not been fully edited. Content may change prior to final publication. Citation information: DOI 10.1109/TIE.2022.3172748, IEEE Transactions on Industrial Electronics

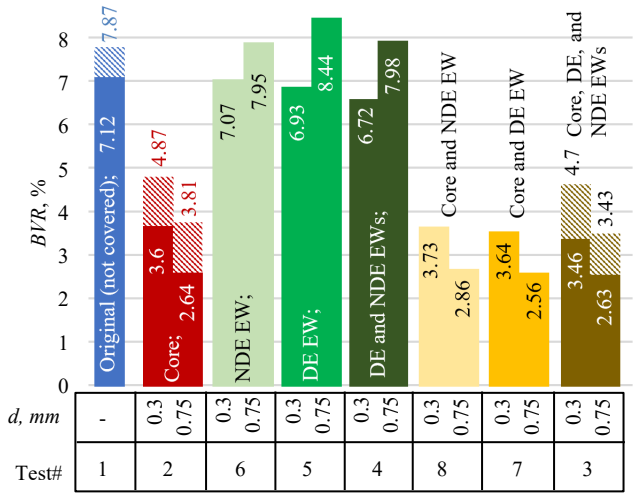

Fig. 9. Averaged *BVR* values were measured at the 15-kW induction machine, when the shielding with a grounded electrode was applied to cover different machine parts. The parts being covered in each test are indicated over the corresponding columns with abbreviations: NDE – "Non-Drive End"; DE – "Drive End", EW – "End Winding". The solid columns show the experimentally observed numbers, and the hatching shows the FEM-calculated *BVR* values for the same cases.

Both simulated and experimental results show that the utilization of the grounded electrodes to cover the core-area obviously brings the main effect in mitigating bearing currents. On the contrary, the coverage of the end-windings only has an insignificant effect. However, the combination of the core-area and winding overhang shielding gives the most effective reduction of *BVR*.

From the experimental data, it can be concluded that the effects of shielding individual parts can be added according to the principle of superposition.

Thus, if we consider for example tests conducted with a 0.3-mm electrode, shielding of the core area-only reduces *BVR* by 3.36 per-cent units, and applying the same countermeasure to both end-windings results in *BVR* = 6.72%, which is 0.56 per-cent units less, than the original value. If we simply calculate the *BVR* of the machine equipped by extended grounded electrodes as a substitution of the effects given by every single action, we observe *BVR* = 7.28%-3.36%-0.56% = 3.36% units. The results of Test#3 show *BVR*=3.46%, which is 3%-units less than the value estimated via using the superposition principle.

Another proof of the viability of the superposition principle can be found if consider Test#4, Test#5, and Test#6 (again, for 0.3 mm electrode as example). When the non-drive end end-winding was shielded, the *BVR* reduces by 0.21 percent units, and when the drive-end end winding was shielded, the *BVR* reduces by 0.36 percent units. The estimated *BVR* of the machine with both end-windings shielded is *BVR* = 7.28% - 0.21% - 0.36% = 6.71%-units. The experimentally found *BVR* for this case is 6.72%, which has an almost perfect match with an estimated number.

It is very interesting to notice, that shielding the drive-end winding overhang brings more effect, than shielding of the non-drive-end one. For the tested 15-kW machine modified with 0.3 mm wire, the shielding of the drive-end winding overhang brings 20% more effect, than the same actions with non-drive-end end-winding does. This can be seen both from the experiments of end-windings only shielding (Tests # 5, 6), and from the combined core-area and end-windings shielding tests (Tests # 7, 8).

An initial explanation of the difference in the bearing current mitigation method impact, most probably, lies in constructive features of the given machine. Even though the machine geometry in theory is considered to be symmetrical at both drive- and non-drive ends, in real motor some asymmetry exists. Thus, the bearings used at different ends of the shaft have slightly different diameter: the drive-end bearing is normally larger in most motors. Larger bearing means larger distance between the raceways, and thus, slightly smaller capacitance of the given bearing. Also, the position of the terminal box and input point of winding supply cables can matter. In the given machine, the terminal box is located close to the drive-end, and the stator winding supply is coming from that side. This can be a reason, why the winding-to-rotor capacitances formed by different end-windings are charged unevenly, with more charge collected at the winding closer to the supply point.

We cannot now proof the superposition principle and discuss about effects of shielding different end-windings with 0.75 mm wires because when these thick slot electrodes are placed, but disconnected, they bring too strong contribution in parasitic capacitances. If we see Test #1 of Table IV, we can find out, that mounted but disconnected system of grounded electrodes increase original *BVR* just by 1.5%. This observation gives us grounds to assume, that relative error of all tests conducted with 0.3 mm electrodes will not exceed this value. But, for case of 0.75 electrodes, the *BVR* of the machine with "inactivated" electrodes is 12.3% higher, than reference value. This is quite significant disadvantage, which will affect the tests. We can see in Tests# 4, 5, and 6, that *BVR* goes even higher, than in original machine. This can be explained by the fact, that being disconnected core-area electrodes acts as a conductive filler of the space between rotor and stator, and increase the parasitic capacitive coupling significantly.

Possible cons of the grounded electrodes introduced into a machine's slot openings were considered in [11]. The same considerations are also applicable for the extended slot electrodes.

Special attention should be paid to the grounding: when the motor is equipped with slot electrodes, but they are not grounded, a small increase of *BVR* can occur, as was noticed in [11]. Negative effect of mounted, but disconnected system, becomes significant with increasing electrode diameter.

The efficiency, torque production and other operating parameters of the machine are not supposed to be compromised, because copper electrodes are nonmagnetic, and do not bring any changes into the magnetic circuit of the machine [27].

As far as the electrodes are connected and collected from one side only without forming closed loops, a squirrel cage is not created, and no extra currents and losses are generated. Since there is no squirrel cage effect, there should be no warries about possible mechanical stress caused by the force acting on the slot electrodes.

Some extra eddy current loss is, of course, possible, but it is negligibly small because of the small thickness of the electrodes.

If consider 3, 15, 75, 110 kW machines presented in Table III, and especially the rightmost column, where extra losses caused by the slot-embedded electrodes are listed, we can find out the following. For the thinnest possible electrodes of 0.1 mm in diameter, mounted to cover the core-area only, the extra eddy-current losses are at the level of 1.48×10^{-7}%, 8.22×10^{-8}%, 4.3×10^{-7}%, 2.88×10^{-8}% from the machine's rated power respectively. For slot electrodes with maximum available diameter for each machine, for 3, 15, 75, 110 kW machines the extra losses are 0.00036%, 0.00054%, 0.00033%, 0.0006% of the machine's rated power respectively.

Joule losses for the case of extended electrodes are naturally slightly higher, but, however, remain in the same order of magnitude.

After all, we see, that in all cases extra losses do not exceed an absolute value of 1 W and remain less than 0.001% from machine rated power. Considering that in all industrial electrical machines the efficiency is normally at the level of 80…98%, and even best motors have losses of several percent, an extra loss of 1 W or less cannot give any arbitrarily notable efficiency drop or anyhow affect the machine performance. Shown extra losses are miserably small and can be considered as more than adequate price for effective reduction of bearing currents.

There are, however, several points that require attention. When the grounded electrodes are extended, reliable insulation between the electrode and the end-winding must be maintained. Placing of the electrodes directly on the winding insulating varnish can cause an earth fault, because the varnish is mainly supposed to provide an interturn insulation. Also, the electrodes must have a good fixation, because possible vibration can cause displacement of freely placed electrodes, which can lead to their fracture or even collision with the rotor.

Slot-embedded electrodes have relatively low capacitance between electrode and winding. It is very good in fighting against non-circulating bearing currents. But, from another hand, this, in theory, might cause small increase in circulating bearing currents. This factor should not be considered in small-scale machines, where non-circulating bearing currents are dominating type of parasitic currents. But in large machines (over 100 kW), where both types of bearing currents can be present, the decision on correct countermeasure to be applied must be done with caution.

Mounting of the slot-embedded electrodes requires invasion inside an electrical machine. Even though it requires just rotor removal, and not requires any serious operations like winding rewound, equipment of the motor with this system cannot be made on site. Therefore, we position this approach as the most suitable option for machine manufacturers or repair workshops, i.e., for those with special equipment and personnel.

VI. Conclusion

Electrostatic shielding by electrodes in slots and also extended to end winding area is studied in electrical machines with varying power. A calculation method was implemented and verified with measurements. It is noticed, that when slot-embedded grounded electrodes are extended to also cover the end-windings, shaft voltage mitigating effect is improved.

In small machines, both core-area and extended electrodes bring a significant reduction of *BVR*. As far as the original *BVR* is very high, maximum efforts must be applied to drop the *BVR* to a safe level. Extended electrodes allow reaching the lowest possible *BVR*.

In a larger machine, e.g., for a 110-kW machine, the desired lowered *BVR* can be reached even with the core-area mounted slot electrodes, when electrodes with a large enough diameter are used. The employment of the extended electrodes allows the desired effect to be achieved using thinner electrodes.

Usage of thinner electrodes is always prioritized, because smaller electrode diameter means smaller eddy current losses, less weight and cost of the electrodes, less complexity of the work.

Applying of extended slot electrodes is a development of the idea introduced before, and this is a natural evolution of the approach. This idea joints the core-area and end-winding-aimed shields.

The *BVR* reduction measures are possible to combine using the superposition principle.

The authors noticed that placing an electrostatic shielding into end windings in drive end is more important, than placing them to non-drive end.

The grounded electrodes offer an effective solution with minimal drawback – minor extra eddy current loss. However, attention must be paid, when the solution is practically applied. Adequate insulation, reliable fixture of the electrodes, good grounding connection, and safe distance to moving parts must be maintained.

Despite the fact that the presented method of suppressing non-circulating bearing currents shows promising results, research tasks in this area still remain. Our future work plans include both further study of the given grounded slot electrode approach and investigating of other bearing current countermeasures.

In the grounded slot electrodes approach, the question of electromagnetic performance remains not studied comprehensively yet, even though loss analysis is carried out in the current paper and theoretical considerations are expressed.

Other research plans are to study some combinations of machine-side countermeasures, develop of the technique for analytical prognosis of the bearing currents at the design stage, and finally declare the combined design rules for creating of bearing-currents-protected electrical machines. Separate research to clarify possible influence of the slot-embedded grounded electrodes on circulating bearing currents should be carried out as well.

References

[1] A. Muetze and A. Binder, "Practical Rules for Assessment of Inverter-Induced Bearing Currents in Inverter-Fed AC Motors up to 500 kW," *IEEE Trans. on Ind. Electron*., vol. 54, no. 3, pp. 1614-1622, Jun. 2007.

[2] T. Zika, I. C. Gebeshuber, F. Buschbeck, G. Preisinger, M. Gröschl, "Surface analysis on rolling bearings after exposure to defined electric stress," in Proceedings of the Institution of Mechanical Engineers, Part J: Journal of Engineering Tribology, vol. 223, issue 5, pp. 787-797, 2009.

[3] J. A. Oliver, G. Guerrero, and J. Goldman, "Ceramic bearings for electric motors: Eliminating damage with new materials," *IEEE Ind. Appl. Mag.*, vol. 23, no. 6, pp. 14–20, Nov./Dec. 2017.

[4] A. Hemati, "A Case Study: Fluting Failure Analysis by Using Vibrations Analysis," Journal of Failure Analysis and Prevention, vol. 19, no. 4, pp. 917–921, 2019.

[5] A. Romanenko, J. Ahola, and A. Muetze, "Influence of electric discharge activity on bearing lubricating grease degradation," 2015 IEEE Energy Conversion Congress and Exposition (ECCE), pp. 4851-4852, 2015.

[6] A. Gonda, R. Capan, D. Bechev, and B. Sauer, "The influence of lubricant conductivity on bearing currents in the case of rolling bearing greases," *Lubricants*, vol. 7, no. 12, Dec. 2019, Art. no. 108.

[7] M. Barnes, *Practical variable speed drives and power electronics*, Newnes, 2003, p. 52.

[8] Renown Electric Motors & Repair inc., "Avoiding Motor Shaft Voltage & Bearing Current Damage," [Online]. Available: https://www.magnetec.de/fileadmin/pdf/bearing-current-damage-guide.pdf/, Accessed: Nov. 07, 2021

[9] K. Vostrov, J. Pyrhönen, and J. Ahola, "Shielding the end windings to reduce bearing currents," in *Proc. Int. Conf. Elect. Mach.*, 2020, pp. 1431–1437.

[10] K. Vostrov, J. Pyrhönen, M. Niemelä, J. Ahola, and P. Lindh, "Mitigating noncirculating bearing currents by a correct stator magnetic circuit and winding design," *IEEE Trans. Ind. Electron.*, vol. 68, no. 5, pp. 3805–3812, May 2021.

[11] K. Vostrov, J. Pyrhönen, P. Lindh, M. Niemelä and J. Ahola, "Mitigation of Inverter-Induced Noncirculating Bearing Currents by Introducing Grounded Electrodes into Stator Slot Openings," *IEEE Trans. Ind. Electron.*, vol. 68, no. 12, pp. 11752–11760, Dec. 2021.

[12] R. F. Schiferl and M. J. Melfi, "Bearing current remediation options," *IEEE Ind. Appl. Mag.*, vol. 10, no. 4, pp. 40-50, Jul./Aug. 2004.

[13] A. Muetze and A. Binder, "Don't lose your bearings," in IEEE Industry Applications Magazine, vol. 12, no. 4, pp. 22-31, July-Aug. 2006.

[14] T. Plazenet, T. Boileau, C. Caironi and B. Nahid-Mobarakeh, "A Comprehensive Study on Shaft Voltages and Bearing Currents in Rotating Machines," *IEEE Ind. Appl. Mag.*, vol. 54, no. 4, pp. 3749-3759, Jul./Aug. 2018.

[15] J. Pyrhönen, V. Hrabovcova, and R. Scott Semken, *Electrical Machine Drives Control: An Introduction*, Hoboken, NJ, USA: Wiley, 2016, ch. 13.

[16] IEC TS 60034-25 Rotating electrical machines – Part 25: AC electrical machines used in power drive systems – Application guide.

[17] A. Binder and A. Muetze, "Scaling Effects of Inverter-Induced Bearing Currents in AC Machines," in *Proc. IEEE Int. Electric Mach. Drives Conf.*, 2007, pp. 1477–1483.

[18] A. Muetze, "Bearing currents in inverter-fed AC-motors," Ph.D. dissertation, Dept. Elect. Comput. Eng., Tech. Univ. Darmstadt, Darmstadt, Germany, 2004.

[19] Y. Xu, Y. Liang, X. Yuan, X. Wu and Y. Li, "Experimental Assessment of High Frequency Bearing Currents in an Induction Motor Driven by a SiC Inverter," *IEEE Access*, vol. 9, pp. 40540-40549, 2021.

[20] H. Prashad, "Effect of operating parameters on the threshold voltages and impedance response of non-insulated rolling element bearings under the action of electrical currents," *Wear*, vol. 117, issue 2, pp. 223–240, June 1987.

[21] A. Muetze and A. Binder, "Practical Rules for Assessment of Inverter-Induced Bearing Currents in Inverter-Fed AC Motors up to 500 kW," *IEEE Trans. Ind. Electron.*, vol. 54, no. 3, pp. 1614-1622, Jun. 2007.

[22] K. Vostrov, J. Pyrhönen, J. Ahola, and M. Niemelä, "Non-circulating bearing currents mitigation approach based on machine stator design options," in Proc. 13th Int. Conf. Elect. Mach., 2018, pp. 866–872.

[23] K. Vostrov, J. Pyrhönen and J. Ahola, "Extension of slot-opening-embedded electrostatic shields in the region of the end-winding to effectively reduce parasitic capacitive coupling," in *Proc. IEEE Int. Electric Mach. Drives Conf.*, 2021, pp. 1-6.

[24] K. Vostrov, J. Pyrhönen, and J. Ahola, "The role of end-winding in building up parasitic capacitances in induction motors," in *Proc. IEEE Int. Electric Mach. Drives Conf.*, 2019, pp. 154–159.

[25] A. Muetze and A. Binder, "Calculation of Motor Capacitances for Prediction of the Voltage Across the Bearings in Machines of Inverter-Based Drive Systems," in *IEEE Trans. Ind. Appl.*, vol. 43, no. 3, pp. 665-672, May/Jun. 2007.

[26] O. Magdun, Y. Gemeinder, and A. Binder, "Prevention of harmful EDM currents in inverter-fed AC machines by use of electrostatic shields in the stator winding overhang," in *Proc. 36th Annu. Conf. IEEE Ind. Electron. Soc.*, 2010, pp. 962–967.

[27] F. J. T. E. Ferreira, M. V. Cistelecan, and A. T. de Almeida, "Evaluation of Slot-Embedded Partial Electrostatic Shield for High-Frequency Bearing Current Mitigation in Inverter-Fed Induction Motors," *IEEE Trans. on Energy Conversion*, vol. 27, no. 2, pp. 382-390, June 2012.

Konstantin Vostrov was born in Leningrad, Russia, in 1991. He received the B.Sc degree in the field of Electrical Engineering, Electromechanics and Electrotechnology from Peter the Great St. Petersburg Polytechnic University in 2014, and the double-degree M.Sc. from the Peter the Great St. Petersburg Polytechnic University in 2015 and Lappeenranta University of Technology in 2016. He is a doctoral student at Lappeenranta–Lahti University of Technology LUT, and his major research interest at the current time is the investigation of the bearing current phenomena in electrical drives and the development of the appropriate countermeasures.

Juha Pyrhönen (M'06), was born in 1957 in Kuusankoski, Finland, received the Doctor of Science (D.Sc.) degree in Electrical Engineering from Lappeenranta University of Technology (LUT), Finland in 1991. He became an Associate Professor of Electrical Engineering at LUT in 1993 and a Professor of Electrical Machines and Drives in 1997. He is engaged in research and development of electric motors and electric drives. His current interests include different synchronous machines and drives, induction motors and drives, and solid-rotor high-speed induction machines and drives.

Markku Niemelä received the B.Sc. degree in electrical engineering from Helsinki Institute of Technology, Helsinki, Finland, in 1990 and the M.Sc. and D.Sc. degrees in technology from Lappeenranta University of Technology (LUT), Lappeenranta, Finland, in 1995 and 1999, respectively. He is currently a Senior Researcher with the Carelian Drives and Motor Centre, LUT. His current interests include motion control, control of line converters, and energy efficiency of electric drives.

Pia Lindh (M'04) born in Helsinki in 1969, received her M.Sc. degree in energy technology in 1998 and her D.Sc. degree in electrical engineering (Technology) in 2004 from Lappeenranta University of Technology (LUT), Lappeenranta, Finland. She is currently serving as an associate professor at the Department of Electrical Engineering in LUT Energy, Lappeenranta, where she is engaged in teaching and research of electric motors and electric drives.

Jero Ahola was born in Lappeenranta, Finland, in 1974. He received the M.Sc. and D.Sc. degrees in electrical engineering from Lappeenranta University of Technology (LUT), Lappeenranta, Finland, in 1999 and 2003, respectively. He is currently Professor of Energy Efficiency in Electrically Driven Systems with the Department of Electrical Engineering, LUT. His research interests include energy efficiency in electrical-motor-driven systems, solar photovoltaic systems, water electrolysis, power-to-X processes, and power-line communication in the motor cables of variable speed electric drives.